Journal of Histochemistry & Cytochemistry 59(6) 591–600

DOI: 10.1369/0022155411404704
http://jhc.sagepub.com
SAGE


# Effect of Immunohistochemistry on Molecular Analysis of Tissue Samples: Implications for Microdissection Technologies

**Michael A. Tangrea, Sumana Mukherjee, Bing Gao, Sanford P. Markey, Qiang Du, Michael Armani, Matthew S. Kreitman, Alex M. Rosenberg, Benjamin S. Wallis, Franziska C. Eberle, Francesca C. Duncan, Jeffrey C. Hanson, Rodrigo F. Chuaqui, Jaime Rodriguez-Canales, and Michael R. Emmert-Buck**

Pathogenetics Unit, Laboratory of Pathology, Center for Cancer Research, National Cancer Institute, National Institutes of Health (NIH), Bethesda, Maryland (MAT,SM,QD,MA,AMR,BSW,FCD,RFC,MRE-B); Laboratory of Neurotoxicology, National Institute of Mental Health, National Institutes of Health, Bethesda, Maryland (BG,SPM); Laser Capture Microdissection Core, Laboratory of Pathology, Center for Cancer Research, National Cancer Institute, NIH, Bethesda, Maryland (MSK,JCH,JR-C); and Hematopathology Section, Center for Cancer Research, National Cancer Institute, NIH, Bethesda, Maryland (FCE).

## Summary

Laser-based tissue microdissection is an important tool for the molecular evaluation of histological sections. The technology has continued to advance since its initial commercialization in the 1990s, with improvements in many aspects of the process. More recent developments are tailored toward an automated, operator-independent mode that relies on antibodies as targeting probes, such as immuno–laser capture microdissection or expression microdissection (xMD). Central to the utility of expression-based dissection techniques is the effect of the staining process on the biomolecules in histological sections. To investigate this issue, the authors analyzed DNA, RNA, and protein in immunostained, microdissected samples. DNA was the most robust molecule, exhibiting no significant change in quality after immunostaining but a variable 50% to 75% decrease in the total yield. In contrast, RNA in frozen and ethanol-fixed, paraffin-embedded samples was susceptible to hydrolysis and digestion by endogenous RNases during the initial steps of staining. Proteins from immunostained tissues were successfully analyzed by one-dimensional electrophoresis and mass spectrometry but were less amenable to solution phase assays. Overall, the results suggest investigators can use immunoguided microdissection methods for important analytic techniques; however, continued improvements in staining protocols and molecular extraction methods are key to further advancing the capability of these methods. (J Histochem Cytochem 59:591–600, 2011)

## Keywords

immunostaining, immunohistochemistry, proteomics, DNA, RNA, tissue microdissection, expression microdissection, immuno-LCM

The field of molecular pathology has advanced over the past 15 years with the integration of laser-based microdissection systems and a variety of associated biological assays and analysis methods (Bonner et al. 1997; Emmert-Buck et al. 1996; Burgess and Hazelton 2000; Iyer and Cox 2010; Craven and Banks 2001; Mustafa et al. 2008; Lawrie and Curran 2005; Charboneau et al. 2002; Gillespie et al. 2004; Bichsel et al. 2001; Callagy et al. 2005; Kurihara et al. 2002). The ability to dissect either morphologically defined cells or discrete geographic regions of a tissue section under microscopic visualization

Submitted October 4, 2010; revised version accepted February 24, 2011

**Corresponding Author:**
Michael R. Emmert-Buck, Pathogenetics Unit, Laboratory of Pathology, Center for Cancer Research, National Cancer Institute, NIH, Bethesda, MD 20892.
Email: mbuck@helix.nih.gov

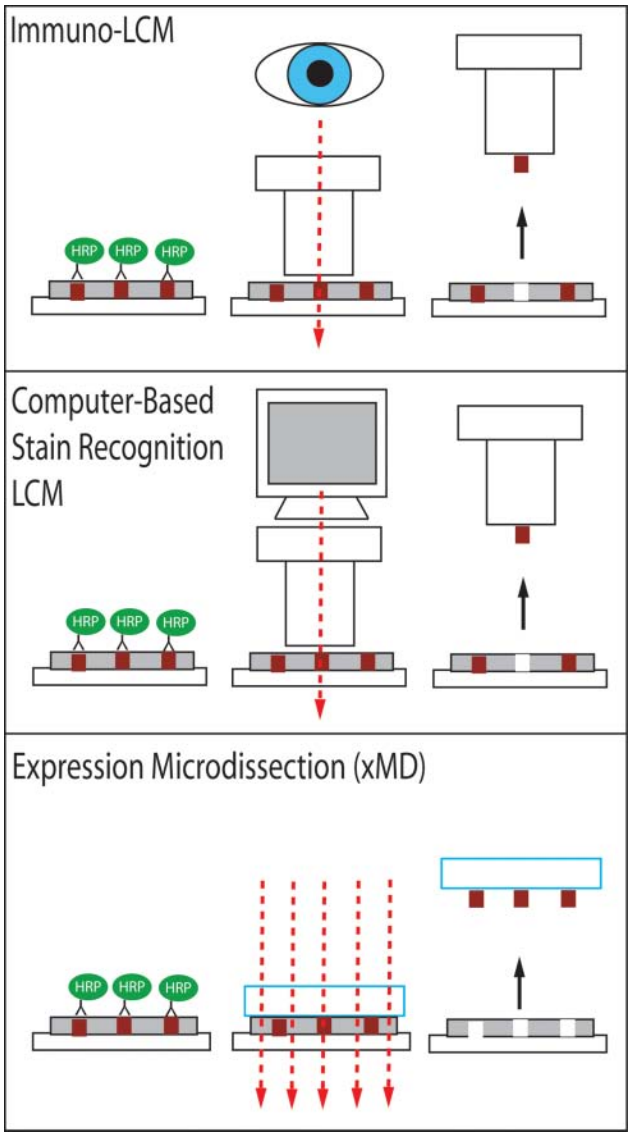


**Figure 1.** Schematic representation of immunoguided microdissection technologies. LCM, laser capture microdissection.

is aiding in the discovery of molecular changes in histological sections, enabling researchers to ask questions that were not technologically feasible in the past. More recently, users have begun employing immunohistochemically stained tissue to guide the dissection process. Several such approaches are in use or in development, including visual immunoguided dissection (immuno–laser capture microdissection [LCM]), computer-based stain recognition software programs, and expression microdissection (xMD) (Fig. 1) (Fend et al. 1999; Eltoum et al. 2002; Tangrea et al. 2004; AutoScanXT Software, Molecular Devices, Sunnyvale, CA). Immunoguided microdissection adds the advantages of increased yield, automation, and the ability to isolate cells or subcellular structures based on functionality/expression rather than purely morphological recognition. Moreover, immunohistochemistry (IHC) can define specific cells or subcellular structures with more precision than standard histochemical staining, offering a finer dissection resolution on the order of ~1 micron in size or less. As an example, xMD uses the 3,3′-diaminobenzidine (DAB) chromogen, used in peroxidase-based IHC, to absorb infrared laser energy, which results in focal heating of an ethylene vinyl acetate (EVA) polymer film in contact with the stained cells (Tangrea et al. 2004). This novel technology provides a high-throughput, user-independent method for biomolecular studies of specific antigen-expressing cells or subcellular structures.

Originally developed in the 1940s and then refined by the incorporation of enzymes in the 1960s, IHC is a valuable tool for histopathological analysis (Nakane and Pierce 1966, 1967; Nakane 1968; Avrameas and Uriel 1966; Coons et al. 1941). Despite some additional modifications made over the years such as the integration of biotin-streptavidin and other labeling enzymes, the technique has remained true to its initial intent, which is to improve visualization of specific antigens within the two-dimensional histology of a tissue section (Cordell et al. 1984; Green 1990; Burnett et al. 1997). From a cell procurement standpoint, standard IHC methods can now be successfully adapted to new immuno-based dissection techniques; however, to date, there has been little assessment of the effects of immunostaining on biomolecule status or recovery. Our recent experiences developing and employing immuno-based dissection methodologies have suggested that the IHC process can negatively affect some biomolecules in tissue sections. To understand this more thoroughly, a variety of tissues (mouse, rat, human) and organs (liver, kidney, prostate, brain, ovary, lymph node) were selected to test the standard IHC protocol and assess biomolecular recovery. Basic quantitative and qualitative downstream analysis methods were employed to systematically evaluate the retrieval of each type of biomolecule (DNA, RNA, protein) following IHC. The study highlights the robustness of DNA and proteins and the labile nature of RNA.

## Materials and Methods

### *Tissue Specimens*

Human, mouse, and rat tissue specimens were used in the study and included the following tissue types: prostate (human), ovarian (human), brain (rat and mouse), lymph node (human), kidney (mouse), and liver (mouse). Biomolecular recovery from formalin-fixed paraffin-embedded (FFPE), ethanol-fixed paraffin-embedded (EFPE), and snap-frozen tissue was examined. Mouse samples were purchased from Pel-Freeze Biologicals (Rogers, AR). Rat tissue was obtained according to National

Institutes of Health (NIH) guidelines. All human specimens were collected under an institutional review board (IRB)–approved protocol and subsequently anonymized.

### *Immunohistochemistry*

A standard IHC protocol using the DAKO Envision$^+$ staining kit (DAKO, Carpinteria, CA) or Invitrogen Histostain Plus DAB kit (Invitrogen, Carlsbad, CA) was used for IHC reactions according to the manufacturer's instructions. For the FFPE tissue, an antigen retrieval step using heat-induced epitope retrieval preceded IHC. Briefly, following dewaxing and rehydration, FFPE tissues were incubated for 20 min in a hot DAKO Antigen Retrieval solution (DAKO). EFPE tissue were dewaxed and rehydrated prior to IHC but not subjected to antigen retrieval. Frozen tissues were fixed in 70% ethanol for 2 min prior to IHC. Primary antibodies for cytokeratin AE1/AE3 (Invitrogen/Zymed, Carlsbad, CA; DAKO), histone H1 (Neomarkers, Fremont, CA), CD31 (BD Pharmigen, San Diego, CA), desmin (Invitrogen/Zymed), and PCNA (Invitrogen/Zymed) were used at a 1:50 dilution with Zymed Antibody Dilutent Solution (Invitrogen/Zymed). Primary and secondary antibody incubation times were 30 min each at room temperature, unless otherwise stated.

### *DNA Analysis*

For DNA quantity and quality measurements, a 12.5-mm$^2$ diameter circle was dissected from frozen ovarian carcinoma tissue using the Veritas LCM machine (Life Technologies, Carlsbad, CA). DNA from dissected tissues was purified using the QIAamp DNA Micro Kit (Qiagen, Valencia, CA) according to the manufacturer's instructions. Purified DNA was quantified using a NanoDrop UV spectrometer (Thermo Scientific, Waltham, MA) at 265 nm. To test DNA integrity, PCR amplification was completed with three different sets of primers for β-globin amplicons of various sizes (152 bp, 268 bp, and 676 bp), as described previously (Gillio-Tos et al. 2007). PCR products were run on a 2% agarose gel and stained with ethidium bromide.

All other DNA analysis studies, such as DNA methylation, are described elsewhere (Grover et al. 2006; Hanson et al. 2006; Rodriguez-Canales et al. 2007). Briefly, immunostained tissue was microdissected via xMD or LCM and then digested with proteinase K overnight. Following lysis and enzyme inactivation at 95C, the DNA was bisulfite modified with the EZ DNA Methlyation Gold kit (Zymo Research, Orange, CA) according to the manufacturer's instructions.

### *RNA Analysis*

RNA quality and quantity were determined using the Agilent BioAnalyzer (Santa Clara, CA) according to the manufacturer's instructions. Commercially available HeLa cell total RNA (Invitrogen) and total human heart RNA (Ambion/Applied Biosystems, Austin, TX) were used for the RNA quality studies. RNA extraction from the tissue specimens was completed using either the Qiagen RNeasy mini kit (Qiagen) or Arcturus Picopure kit (Life Technologies) according to the manufacturer's instructions. RNA samples were quantified by NanoDrop UV spectrometer, and subsequent TaqMan analysis was carried out on an Applied Biosystems 7500 Fast Real-Time PCR System (Applied Biosystems, Foster City, CA) according to the manufacturer's instructions.

### *Protein Analysis*

1D-PAGE of frozen immunostained human prostate tissue scrapes was completed on 4% to 20% Tris-Glycine gels (Invitrogen) at 125 V for 1.5 hr. The 1D-PAGE gels were stained using Microwave Blue (Protiga, Frederick, MD) according to the manufacturer's instructions. For 2D-PAGE analysis, eight frozen mouse liver sections were immunostained for smooth muscle actin via a peroxidase-based staining method. Following staining, the tissues were scraped from the glass slides and placed in ToPI-PAGE Buffer (ITSI Biosciences, Johnstown, PA) with protease inhibitor cocktail (GE Healthcare/Amersham Biosciences, Piscataway, NJ). Eight unstained frozen mouse liver sections were used as a control sample. 2D-PAGE analysis was completed with the Ettan IPG Phor system (GE Healthcare) and the pH 3–10 gel strip according to the manufacturer's instructions.

For Western blot analysis, frozen mouse liver, kidney, and brain tissue were cryo-sectioned at 10 μm onto charged glass slides. The sections were fixed briefly in 70% ethanol. The unstained sections were then scraped and transferred to an Eppendorf tube. The stained sections went through an immunohistochemistry protocol for mouse anti–histone H1 (1:50 dilution; Abcam) as described above. The stained and unstained sections were then placed in a SDS Tris-Glycine sample buffer with β-mercaptoethanol and heated to 95C for 10 min. For the microdissected Western blot, a circular tissue area of 12.5 mm$^2$ was dissected via LCM on the Arcturus XT machine (Life Technologies). Following dissection, the films were removed from the LCM caps and placed in the SDS Tris-Glycine buffer with β-mercaptoethanol. Multiple caps were combined to generate the sample areas, either 50 mm$^2$ or 25 mm$^2$. The microdissected samples were gently heated at 60C for 10 min to prevent melting of the LCM film during lysis. The samples were centrifuged at full speed for 10 min, and then the supernatant was loaded onto a 4% to 20% Tris-Glycine gel. The samples were electrophoresed at 125 V for 1.5 hr. The separated proteins were then transferred to a PVDF membrane via the iBlot system (Invitrogen) according to the manufacturer's instructions. A rabbit anti–proliferating

cell nuclear antigen (PCNA) antibody (1:200 dilution; Abcam) was used to probe the PVDF membrane using the TMB Western Blot Kit (KPL, Inc., Gaithersburg, MD) for blocking and detection according to the manufacturer's instructions. 3T3 cell lysate (ProSci Incorporated, Ponway, CA) was used as a control for PCNA as recommended by the antibody manufacturer.

For mass spectrometry, microdissected cells were lysed in 50 µL of trifluoroethanol (TFE)/50 mM ammonium bicarbonate (1:1, v:v) and then sonicated in a water bath for 20 min (Wang et al. 2005; Liebler and Ham 2009). Samples were reduced with dithiothreitol (10 mM) at 50C for 15 min followed by alkylation with iodoacetamine (20 mM) in the dark at room temperature for 15 min. The buffer was adjusted to 250 µL (containing 10% TFE and pH adjustment for trypsin to 8.0) and tryptic digestion performed at 37C overnight. The digests were resuspended in 5% acetonitrile, 0.1% formic acid for liquid chromatography/mass spectrometry (LC/MS/MS) analysis. Tryptic peptides were injected into a Nano LC 1D Proteomics HPLC system (Eksigent, Dublin, CA) coupled online to an (LTQ)-Orbitrap mass spectrometer equipped with a Nanomate nanoelectrospray ionization source (Advion, Ithaca, NY). Upon injection, all peptide samples were desalted and preconcentrated online with a nano-C18 precolumn (300 mM × 5 mm) and then separated using a 75 mm × 10 cm BetaBasic-18 PicoFrit analytical column (New Objective, Woburn, MA) connected to the nanospray source. A linear gradient was developed using a 400-nl/min flow rate. LC mobile phases were A: 95% water/5% acetonirile/0.1% formic acid and B: 20% water/80% acetonitrile/0.1% formic acid. Retained analytes were eluted by increasing the acetonitrile concentration to 60% or 1.25% per min. All 1D LC/MS/MS experiments were operated such that spectra were acquired for 60 min in the data-dependent mode with dynamic exclusion enabled. The top five peaks in the 400- to 2000-m/z range of every MS survey scan were fragmented. Survey spectra were acquired with 60,000 resolutions in the Orbi-mass analyzer and fragmented in the LTQ ion trap. The spectra were analyzed using MASCOT searching engine against the Swissprot database. The precursor ion tolerance was set to 0.1 Da, whereas fragment ion tolerance was 0.8 Da. Candidate peptides were required to possess tryptic termini at both ends and allowed a maximum of one missed cleavage. A final list of protein identifications was created adhering to the parsimony principle, reporting a minimal number of protein identifications from a pool of uniquely identified peptides.

## Results and Discussion

### *DNA Analysis*

The status of DNA in immunostained histological sections depends heavily on the upstream tissue processing steps. In general, snap-frozen tissue sections contain high-quality, relatively intact DNA that is amenable to a full range of analysis techniques, including Southern blots, PCR, and array-based technologies (Frost et al. 2001; Reynolds and Diehl 1993). EFPE tissue also has relatively large, intact DNA, although the quantity recovered is reduced compared to frozen tissue specimens (Gillespie et al. 2002). In contrast, FFPE tissue contains fragmented DNA due to the effects of formalin fixation; however, these samples can be analyzed by PCR, sequencing, and arrays if the conditions are adapted for smaller sized DNA pieces (Wood et al. 2010).

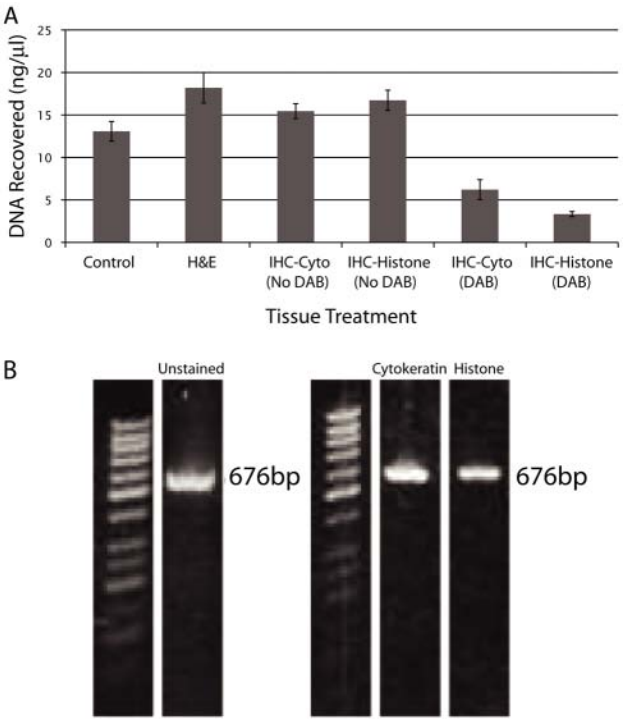


**Figure 2.** DNA analysis following immunostaining. (A) DNA concentrations following immunohistochemistry (IHC) of frozen ovarian carcinoma. DNA was purified prior to determination of concentration. Control is unstained tissue. (B) PCR amplification of a 676-bp amplicon of β-globin from immunostained frozen ovarian tissue. DAB, 3,3′-diaminobenzidine; H&E, hematoxylin and eosin.

Overall, the data indicate that DNA is the most robust biomolecule for use with the new expression-based dissection systems and is affected the least by the IHC process. DNA remains stable during IHC, and the quality is essentially the same before and after the staining process. Using PCR amplification of β-globin, the integrity of DNA was not affected by IHC; however, DNA quantity was diminished (Fig. 2). Evaluating the DNA quantity recovered from frozen immunostained breast, ovarian, and prostate tissue, the amount recovered was diminished by ~50% to 75% of the amount recovered from unstained tissue from the same

case. The reduction in DNA from tissue sections after IHC is more pronounced after staining of nuclei, such as with anti–histone H1, when compared to cytoplasmic staining with cytokeratin AE1/AE3 (Fig. 2A). This effect is most likely due to problems in DNA recovery as opposed to DNA damage because the quality of the DNA was not affected during the staining process, suggesting that the higher concentration of DAB stain in the local vicinity of the genomic DNA interfered in subsequent extraction steps.

Despite the diminished recovery, DNA from immunostained tissue is amplifiable by PCR, with no obvious difference in performance between IHC-stained and unstained samples (Fig. 2B). Beta-globin PCR amplicons of various sizes (152 bp, 268 bp, and 676 bp) were produced from purified frozen ovarian tumor DNA samples, thus indicating that the quality of DNA recovered from immunostained tissue is sufficient for successful amplification, including relatively large amplicons of up to 676 bp in length. These results are consistent with several other studies in our group (Eberle et al. 2010; Grover et al. 2006; Hanson et al. 2006). For example, it was previously shown that xMD samples could be evaluated for DNA methylation status via pyrosequencing (Grover et al. 2006; Hanson et al. 2006), demonstrating that DNA recovered from immunostained EFPE samples, both stromal and endothelial cells, produced accurate genomic sequencing after bisulfite modification and PCR amplification. Similarly, our laboratory used immuno-LCM to recover stromal cells for DNA methylation analysis of EFPE human prostate tissue in an epigenetic, anatomical mapping project (Rodriguez-Canales et al. 2007), and no significant adverse effects from IHC on the quality of the DNA recovered were observed. Finally, we were able to establish an optimized protocol for antigen retrieval (AR) and IHC of FFPE specimens suitable for immuno-LCM and DNA methylome analysis using a high-throughput array (Eberle et al. 2010). DNA from microdissected cells of immunohistochemically or hematoxylin and eosin (H&E)–stained tissue sections showed identical DNA quality and a strong correlation ($r$ = 0.94–0.98) for CpG target methylation of 1505 sites in a series of five paired lymphoid samples (Eberle et al. 2010). Taken together, these results demonstrate the ability to successfully analyze DNA recovered from immunostained tissue sections. To date, the main drawback is the reduced DNA yields from these samples, a difficulty that can be mitigated by the use of PCR to amplify recovered DNA and one that is counterbalanced by the increased speed and/or precision of probe-based dissection.

## *RNA Analysis*

Similar to DNA, RNA is generally of high quality in frozen tissue sections and is fragmented in both FFPE and EFPE samples (Benchekroun et al. 2004; Okello et al. 2010; Farragher et al. 2008; Penland et al. 2007; von Ahlfen et al. 2007; Perlmutter et al. 2004). However, in contrast to DNA, the stability of RNA during the immunostaining procedure is markedly reduced in frozen and EFPE samples due to endogenous tissue RNases that become active during the staining process. The conundrum for investigators is that aqueous buffer conditions used for immunostaining are also favorable for RNase activity, making it difficult to simultaneously stain tissue and protect the RNA. Numerous attempts by our group and others to address this challenge have met with only limited success (Brown and Smith 2009; von Smolinski et al. 2006). For example, modifying the IHC process by shortening the incubation steps and decreasing the time for IHC to as little as 15 min, compared to the standard 90-min protocol, did not significantly improve yields. In parallel with shortening incubation times, RNase inhibitors such as RNase OUT or ribonucleaside vanadyl complex were also added to the incubation solutions and evaluated. Other approaches tested included using RNA-preserving products such as RNAlater ICE, RNase Away, and pretreatment of the tissue with acetone, as well as protein cross-linkers and cysteine-cysteine reducing agents to decrease endogenous RNase activity. Overall, these approaches and those reported by other groups provided only minimal positive benefit in preserving RNA quality and quantity during IHC and have not proven universally successful with a broad range of antibodies and tissue types. At present, most studies of RNA after immunostaining are limited to RT-PCR analysis of small amplicons or alternatively are performed on tissues with low levels of endogenous RNase activity such as brain (Macdonald et al. 2008; Fassunke et al. 2004; Jin et al. 2001; Fend et al. 1999).

A systematic analysis of RNA during IHC illustrates that significant degradation occurs throughout the entire process. Moreover, because IHC methods were developed for tissue staining and visualization, many standard reagents are not RNase free, an issue that needs to be considered when using commercial immuno-based kits for studies that include a subsequent RNA analysis component. For example, as shown in Figure 3A, HeLa cell line total RNA incubated with primary antibody solution resulted in degradation of the 18s and 28s rRNA bands within 20 min, indicating the primary antibody solution itself demonstrated RNase activity. Next, the effects of endogenous tissue RNases during each wash and incubation step of IHC were assessed. As seen in Figure 3B, significant degradation of RNA by endogenous RNases occurs continuously over time, and within 5 min, there is no visible rRNA. RNA displayed signs of degradation as early as the initial wash step with PBS, and additional hydrolysis was observed at each subsequent IHC stage. In an attempt to reduce RNA fragmentation, we performed immunostaining of a tissue section with diethylpyrocarbonate (DEPC)–treated water in place of standard RNase-free PBS. The 18s and 28s bands of rRNA

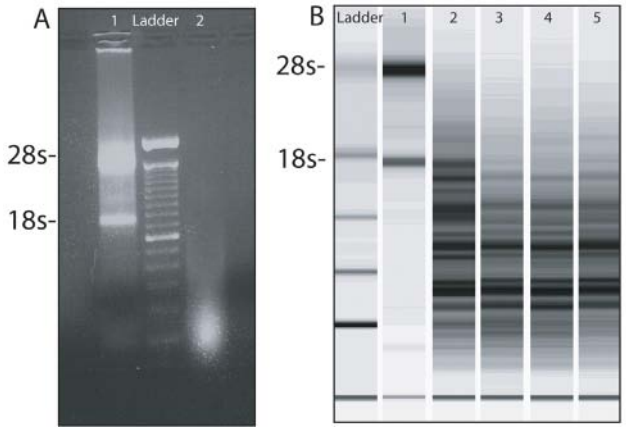


**Figure 3.** RNA analysis following immunostaining. (A) An agarose gel of 5 µg HeLa total RNA (lane 1) and 5 µg HeLa total RNA incubated with primary antibody for anti–cytokeratin AE1/AE3 for 20 min (lane 2). (B) A BioAnalyzer image of total RNA from a frozen tissue section (lane 1), after three quick washes in PBS (lane 2), after antibody solution for 5 min (lane 3), after 5-min 3,3′-diaminobenzidine (DAB) incubation (lane 4), and after 2-min DAB enhancer incubation (lane 5).

were retained after IHC; however, the procedure failed to stain the tissue due to the inability of the primary antibody to bind its antigen in a non-buffered solution (data not shown). This result again highlights the difficulty in identifying experimental conditions for tissue sections that are favorable for immunostaining but at the same time unfavorable for RNase activity.

In contrast to frozen and EFPE tissue samples, FFPE specimens may be uniquely applicable for immunoguided mRNA studies in the future, especially when high-throughput methods such as auto-recognition dissection software or xMD are employed to procure a sizable number of cells. In fact, this may prove to be a particularly important and valuable capability of probe-based microdissection. Traditionally, investigators have analyzed RNA in FFPE tissue by starting with relatively large amounts of non-microdissected tissue—multiple serial microtome sections, for example, thereby creating enough medium- and large-size mRNA fragments for successful analysis (Roberts et al. 2009). However, this strategy is problematic for standard dissection studies because there are practical limitations to the number of cells that can be procured. The potential advantage of FFPE specimens for immunoguided microdissection is that endogenous tissue RNases may become entrapped in a meshwork of crosslinked proteins during formalin fixation, possibly rendering them inactive, allowing for improved RNA preservation during IHC. Because expression-based dissection technologies enable one to dissect significantly more cells (an order of magnitude or more) than typical phenotype-based microdissection, we propose that it may allow for RNA to be obtained from FFPE tissue, making this a promising approach for future gene expression studies of archival pathology specimens.

## *Protein Analysis*

In the present study, our focus was on the recovery and analysis of proteins from immunostained frozen tissue sections using 1D-PAGE, Western blot, 2D-PAGE, and mass spectrometry. Overall, the data show that IHC affects subsequent protein recovery for some but not all methods. At the outset, we were concerned that the exogenously added primary and secondary antibodies used for immunostaining would be major contaminants and interfere with downstream methods, perhaps requiring an antibody removal step prior to analysis. However, this was not the case, and the primary and secondary antibodies used for IHC were not problematic, suggesting the mass amount of antibody that binds to tissue during IHC is less than expected (data not shown).

We initially analyzed frozen human prostate tissue using 1D-PAGE and found that proteins can be successfully analyzed by denaturing electrophoresis and are of generally good quality following immunostaining (Fig. 4A). However, the quantity of recovered protein varies depending on the method used for immunostaining, colorimetric versus fluorescent. Other laboratories have had similar observations and switched from a horseradish peroxidase–based approach to an alkaline phosphatase system (Lu et al. 2008). At present, use of fluorescent staining and auto-recognition software is the preferred staining approach (Fig. 4A); however, colorimetric staining is effective for many xMD-based studies, and efforts to replace DAB with immunogold targeting or other nanoparticles are in progress.

In addition, we evaluated the immunostaining effect on various frozen mouse tissue specimens (liver, kidney, and brain) for Western blotting analysis. All three tissues were subjected to colorimetric IHC staining for histone H1, a ubiquitous nuclear marker. Following IHC, the tissue was lysed and probed via Western blot for PCNA (Fig. 4B). Although a PCNA band was detected, a somewhat diminished signal was observed in the IHC-stained tissue samples as compared to unstained tissue (Fig. 4B, top). This decrease was observed even though equal amounts of protein were loaded within each tissue group. To investigate further, we LCM dissected mouse liver specimens that were either unstained or immunostained (Fig. 4B, bottom). Interestingly, the microdissected samples did not exhibit as pronounced a difference in band intensity between stained and unstained tissue when compared to the scraped tissue samples. This phenomenon may be due to the accessibility of the lysis buffer to the microdissected tissue on the LCM capture film. The data show that Western blotting is possible with immunostained tissue, although the user may need to adjust the amount of protein

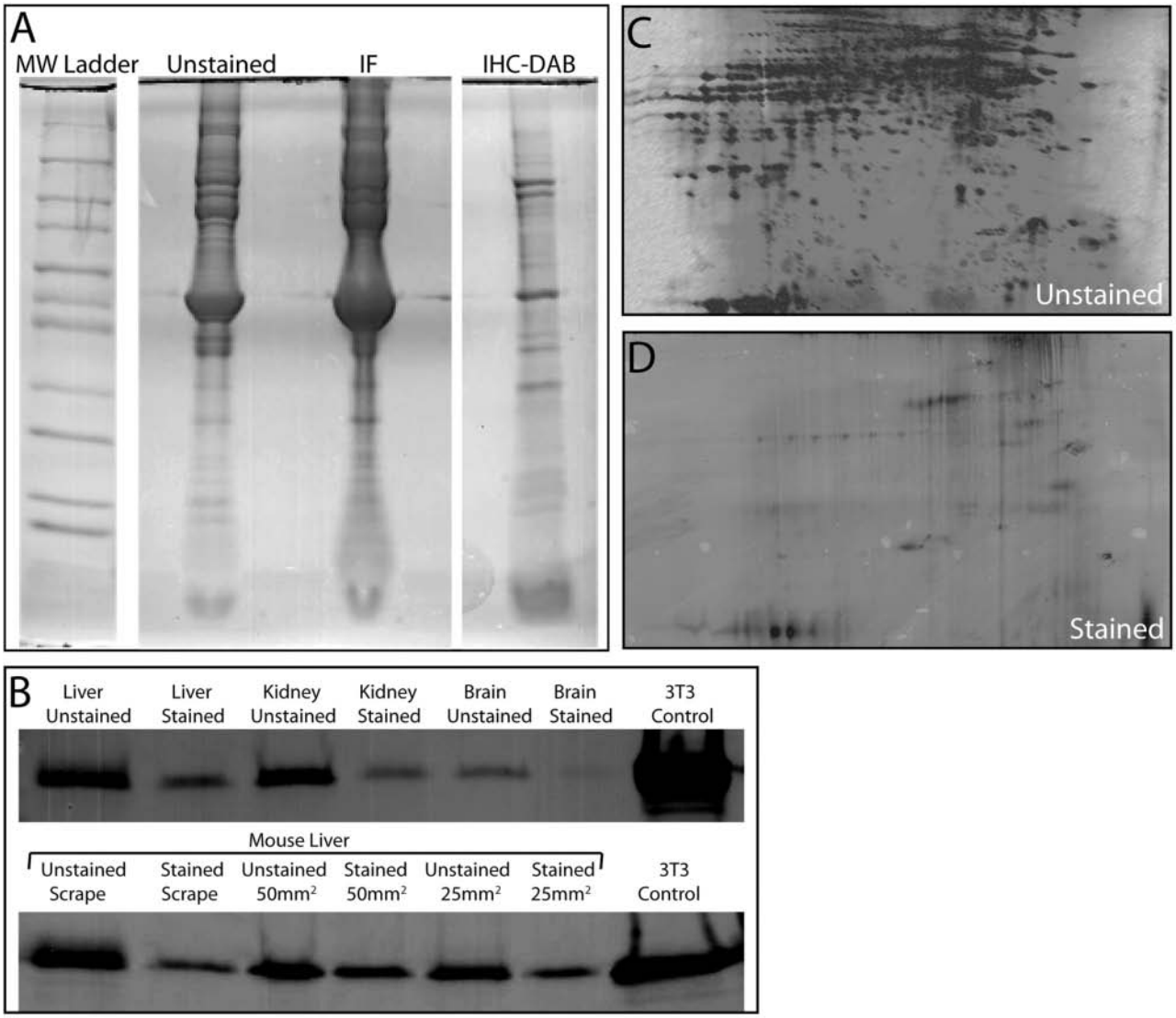


**Figure 4.** Protein analysis following immunostaining. (A) 1D-PAGE of frozen human prostate tissue either without staining or following immunofluorescence (IF) or immunohistochemistry–3,3′-diaminobenzidine (IHC-DAB) staining. (B) Western blots of frozen mouse tissue samples before and after IHC-DAB (top) or mouse liver tissue microdissected before or after IHC-DAB (bottom). The total area of laser capture microdissection (LCM) dissected tissue is listed where appropriate. In both Western blots (top and bottom), the stained tissue was targeted via IHC-DAB for anti–histone H1, and the Western membrane was probed for proliferating cell nuclear antigen (PCNA) with a detected molecular weight of 29 kDa. (C) Silver-stained mouse liver lysate 2D-PAGE. (D) Silver-stained mouse liver lysate following immunostaining.

lysate loaded onto the 1D-PAGE gel to detect a band, especially when targeting low abundant proteins.

The most pronounced difficulty observed for protein studies after immunostaining is with methods that require solubilization of the protein content in a relatively gentle extraction buffer, solution phase immunoassays or 2D-PAGE as examples, as the proteins appear compromised to some extent. The first dimension of 2D-PAGE uses a mild lysis buffer to maintain the pI of the proteins for isoelectrical focusing, and the mild buffer is unable to solubilize the majority of proteins following IHC. As shown in Figure 4C,D, the amount of detectable proteins in IHC-stained frozen mouse liver tissue was only a small fraction of that observed when an unprocessed section was evaluated.

In contrast to solution phase assays, mass spectrometry appears to be an effective analysis system for immunoguided dissection studies. An important advantage here is that harsh chemicals and treatments are typically used to dissociate and digest proteins into peptide fragments, allowing the proteome to be studied following IHC. Thus, proteins

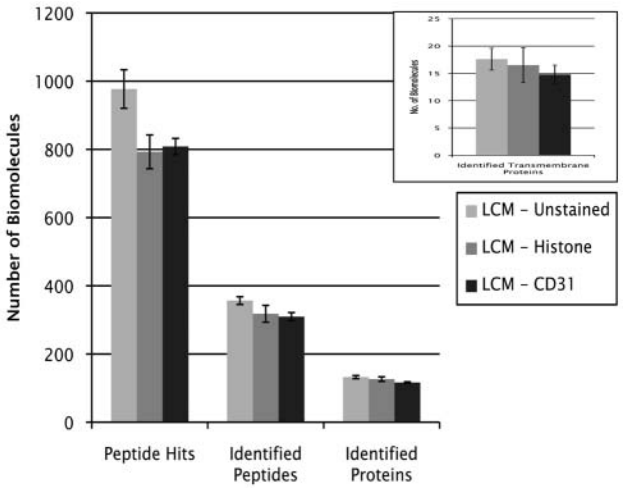


**Figure 5.** Proteomic analysis of immunostained and unstained, microdissected frozen rat brain tissue. Graphical representation of data generated using an LTQ-Orbitrap and SwissProt Rattus database. Immunohistochemical staining was completed for histone H1 and CD31 antigens using a standard 90-min immunohistochemistry–3,3′-diaminobenzidine (IHC-DAB) protocol. LCM, laser capture microdissection.

that are not easily recovered in mild solutions can be resolved after digestion to peptides. The results to date indicate there is little difference (<10%) in mass spectrometry results between unstained tissue and immunostained tissue for nuclei (anti–histone H1) or blood vessels (anti-CD31) from microdissected, frozen rat brain tissue (Fig. 5). These results suggest that mass spectrometry is the method of choice for proteomic analysis of immunostained tissue.

## Future Directions

The field of molecular pathology is continually advancing due to improvements in analysis technologies. Laser-based dissection, automated immunostaining, multiplex fluorescent probe systems, layered expression scanning (LES), and spectral imaging all offer new possibilities for the study of histological sections (Gannot et al. 2007; Grogan 1992). Importantly, the capability of each new approach must be matched to the specific needs of a given study, and investigators must consider the strengths, weaknesses, and optimal use of the methodologies. Next-generation, target-based microdissection technologies have the potential to advance the molecular pathology field by improving dissection speed and precision; however, they also have limitations and drawbacks depending on the biomolecule(s) to be analyzed.

The present study assessed biomolecule status in immunostained sections and identified assay methods that can be used in the near term, as well as areas where improvements in protocols or strategy are needed. We found that DNA and proteins are more easily recovered following IHC, whereas RNA degrades quickly during the initial staining steps, and thus the success of downstream analysis methods is highly dependent on the integrity of the biomolecules after immunostaining.

The current data sets also highlight an important aspect of all microdissection-based work—namely, it is preferable to compare "like versus like" in studies of dissected cell populations whenever possible. In other words, studying two cell types from the same histological section will correct for molecular changes and normalize technical artifacts associated with tissue and slide handling as the cells have gone through identical processing conditions. Looking forward, continued improvement of these and other methodologies likely will further the vital role of tissue-based analysis in many aspects of biomedical research, including gene discovery efforts, clinical assays, and the study of tissue from animal model systems.

### Declaration of Conflicting Interests

MAT, RFC, and MRE-B are inventors on NIH held patents covering microdissection technologies and can receive royalty-based payments through the NIH technology transfer system.

### Funding

The author(s) disclosed receipt of the following financial support for the research and/or authorship of this article: This research was supported in part by the intramural program of the NIH, National Cancer Institute, Center for Cancer Research.

### References

Avrameas S, Uriel J. 1966. Method of antigen and antibody labelling with enzymes and its immunodiffusion application [in French]. C R Acad Sci Hebd Seances Acad Sci D. 262:2543–2545.

Benchekroun M, Degraw J, Gao J, Sun L, Von Boguslawsky K, Leminen A, Andersson LC, Heiskala M. 2004. Impact of fixative on recovery of mRNA from paraffin-embedded tissue. Diagn Mol Pathol. 13:116–125.

Bichsel VE, Liotta LA, Petricoin EF III. 2001. Cancer proteomics: from biomarker discovery to signal pathway profiling. Cancer J. 7:69–78.

Bonner RF, Emmert-Buck M, Cole K, Pohida T, Chuaqui R, Goldstein S, Liotta LA. 1997. Laser capture microdissection: molecular analysis of tissue. Science. 278:1481–1483.

Brown AL, Smith DW. 2009. Improved RNA preservation for immunolabeling and laser microdissection. RNA. 15:2364–2374.

Burgess JK, Hazelton RH. 2000. New developments in the analysis of gene expression. Redox Rep. 5:63–73.

Burnett R, Guichard Y, Barale E. 1997. Immunohistochemistry for light microscopy in safety evaluation of therapeutic agents: an overview. Toxicology. 119:83–93.

Callagy G, Jackson L, Caldas C. 2005. Comparative genomic hybridization using DNA from laser capture microdissected tissue. Methods Mol Biol. 293:39–55.

Charboneau L, Tory H, Chen T, Winters M, Petricoin EF III, Liotta LA, Paweletz CP. 2002. Utility of reverse phase protein arrays: applications to signalling pathways and human body arrays. Brief Funct Genomic Proteomic. 1:305–315.

Coons AH, Creech HJ, Jones RN. 1941. Immunological properties of an antibody containing a fluorescent group. Proc Soc Exp Biol Med. 47:200–202.

Cordell JL, Falini B, Erber WN, Ghosh AK, Abdulaziz Z, Macdonald S, Pulford KA, Stein H, Mason DY. 1984. Immunoenzymatic labeling of monoclonal antibodies using immune complexes of alkaline phosphatase and monoclonal anti-alkaline phosphatase (APAAP complexes). J Histochem Cytochem. 32:219–229.

Craven RA, Banks RE. 2001. Laser capture microdissection and proteomics: possibilities and limitation. Proteomics. 1:1200–1204.

Eberle FC, Hanson JC, Killian JK, Wei L, Ylaya K, Hewitt SM, Jaffe ES, Emmert-Buck MR, Rodriguez-Canales J. 2010. Immuno-guided laser assisted microdissection technique for DNA methylation analysis of archival tissue specimens. J Mol Diagn. 12:394–401.

Eltoum IA, Siegal GP, Frost AR. 2002. Microdissection of histologic sections: past, present, and future. Adv Anat Pathol. 9:316–322.

Emmert-Buck MR, Bonner RF, Smith PD, Chuaqui RF, Zhuang Z, Goldstein SR, Weiss RA, Liotta LA. 1996. Laser capture microdissection. Science. 274:998–1001.

Farragher SM, Tanney A, Kennedy RD, Paul Harkin D. 2008. RNA expression analysis from formalin fixed paraffin embedded tissues. Histochem Cell Biol. 130:435–445.

Fassunke J, Majores M, Ullmann C, Elger CE, Schramm J, Wiestler OD, Becker AJ. 2004. In situ–RT and immunolaser microdissection for mRNA analysis of individual cells isolated from epilepsy-associated glioneuronal tumors. Lab Invest. 84:1520–1525.

Fend F, Emmert-Buck MR, Chuaqui R, Cole K, Lee J, Liotta LA, Raffeld M. 1999. Immuno-LCM: laser capture microdissection of immunostained frozen sections for mRNA analysis. Am J Pathol. 154:61–66.

Frost AR, Eltoum IE, Siegal GP. 2001. Laser capture microdissection. Curr Protoc Mol Biol. Chapter 25:Unit 25A.1.

Gannot G, Tangrea MA, Richardson AM, Flaig MJ, Hewitt SM, Marcus EM, Emmert-Buck MR, Chuaqui RF. 2007. Layered expression scanning: multiplex molecular analysis of diverse life science platforms. Clin Chim Acta. 376:9–16.

Gillespie JW, Best CJ, Bichsel VE, Cole KA, Greenhut SF, Hewitt SM, Ahram M, Gathright YB, Merino MJ, Strausberg RL, et al. 2002. Evaluation of non-formalin tissue fixation for molecular profiling studies. Am J Pathol. 160:449–457.

Gillespie JW, Gannot G, Tangrea MA, Ahram M, Best CJ, Bichsel VE, Petricoin EF, Emmert-Buck MR, Chuaqui RF. 2004. Molecular profiling of cancer. Toxicol Pathol. 32(suppl 1):67–71.

Gillio-Tos A, De Marco L, Fiano V, Garcia-Bragado F, Dikshit R, Boffetta P, Merletti F. 2007. Efficient DNA extraction from 25-year-old paraffin-embedded tissues: study of 365 samples. Pathology. 39:345–348.

Green NM. 1990. Avidin and streptavidin. Methods Enzymol. 184:51–67.

Grogan TM. 1992. Automated immunohistochemical analysis. Am J Clin Pathol. 98:S35–S38.

Grover AC, Tangrea MA, Woodson KG, Wallis BS, Hanson JC, Chuaqui RF, Gillespie JW, Erickson HS, Bonner RF, Pohida TJ, et al. 2006. Tumor-associated endothelial cells display GSTP1 and RARbeta2 promoter methylation in human prostate cancer. J Transl Med. 4:13.

Hanson JA, Gillespie JW, Grover A, Tangrea MA, Chuaqui RF, Emmert-Buck MR, Tangrea JA, Libutti SK, Linehan WM, Woodson KG. 2006. Gene promoter methylation in prostate tumor-associated stromal cells. J Natl Cancer Inst. 98:255–261.

Iyer EP, Cox DN. 2010. Laser capture microdissection of Drosophila peripheral neurons. J Vis Exp. May 24;(39):pii 2016.

Jin L, Tsumanuma I, Ruebel KH, Bayliss JM, Lloyd RV. 2001. Analysis of homogeneous populations of anterior pituitary folliculostellate cells by laser capture microdissection and reverse transcription-polymerase chain reaction. Endocrinology. 142:1703–1709.

Kurihara Y, Ghazizadeh M, Bo H, Shimizu H, Kawanami O, Moriyama Y, Onda M. 2002. Genome-wide screening of laser capture microdissected gastric signet-ring cell carcinomas. J Nippon Med Sch. 69:235–242.

Lawrie LC, Curran S. 2005. Laser capture microdissection and colorectal cancer proteomics. Methods Mol Biol. 293:245–253.

Liebler DC, Ham AJ. 2009. Spin filter-based sample preparation for shotgun proteomics. Nat Methods. 6:785; author reply 785–786.

Lu Q, Murugesan N, Macdonald JA, Wu SL, Pachter JS, Hancock WS. 2008. Analysis of mouse brain microvascular endothelium using immuno-laser capture microdissection coupled to a hybrid linear ion trap with Fourier transform-mass spectrometry proteomics platform. Electrophoresis. 29:2689–2695.

Macdonald JA, Murugesan N, Pachter JS. 2008. Validation of immuno-laser capture microdissection coupled with quantitative RT-PCR to probe blood-brain barrier gene expression in situ. J Neurosci Methods. 174:219–226.

Mustafa D, Kros JM, Luider T. 2008. Combining laser capture microdissection and proteomics techniques. Methods Mol Biol. 428:159–178.

Nakane PK. 1968. Simultaneous localization of multiple tissue antigens using the peroxidase-labeled antibody method: a study on pituitary glands of the rat. J Histochem Cytochem. 16:557–560.

Nakane PK, Pierce GB Jr. 1966. Enzyme-labeled antibodies: preparation and application for the localization of antigens. J Histochem Cytochem. 14:929–931.

Nakane PK, Pierce GB Jr. 1967. Enzyme-labeled antibodies for the light and electron microscopic localization of tissue antigens. J Cell Biol. 33:307–318.

Okello JB, Zurek J, Devault AM, Kuch M, Okwi AL, Sewankambo NK, Bimenya GS, Poinar D, Poinar HN. 2010. Comparison of

methods in the recovery of nucleic acids from archival formalin-fixed paraffin-embedded autopsy tissues. Anal Biochem. 400:110–117.

Penland SK, Keku TO, Torrice C, He X, Krishnamurthy J, Hoadley KA, Woosley JT, Thomas NE, Perou CM, Sandler RS, et al. 2007. RNA expression analysis of formalin-fixed paraffin-embedded tumors. Lab Invest. 87:383–391.

Perlmutter MA, Best CJ, Gillespie JW, Gathright Y, Gonzalez S, Velasco A, Linehan WM, Emmert-Buck MR, Chuaqui RF. 2004. Comparison of snap freezing versus ethanol fixation for gene expression profiling of tissue specimens. J Mol Diagn. 6:371–377.

Reynolds JE, Diehl SR. 1993. A method for recovery of high-molecular-weight DNA suitable for field-inversion gel electrophoresis from frozen tumor cells. Cancer Genet Cytogenet. 65:68–70.

Roberts L, Bowers J, Sensinger K, Lisowski A, Getts R, Anderson MG. 2009. Identification of methods for use of formalin-fixed, paraffin-embedded tissue samples in RNA expression profiling. Genomics. 94:341–348.

Rodriguez-Canales J, Hanson JC, Tangrea MA, Erickson HS, Albert PS, Wallis BS, Richardson AM, Pinto PA, Linehan WM, Gillespie JW, et al. 2007. Identification of a unique epigenetic sub-microenvironment in prostate cancer. J Pathol. 211:410–419.

Tangrea MA, Chuaqui RF, Gillespie JW, Ahram M, Gannot G, Wallis BS, Best CJ, Linehan WM, Liotta LA, Pohida TJ, et al. 2004. Expression microdissection: operator-independent retrieval of cells for molecular profiling. Diagn Mol Pathol. 13:207–212.

von Ahlfen S, Missel A, Bendrat K, Schlumpberger M. 2007. Determinants of RNA quality from FFPE samples. PLoS One. 2:e1261.

von Smolinski D, Blessenohl M, Neubauer C, Kalies K, Gebert A. 2006. Validation of a novel ultra-short immunolabeling method for high-quality mRNA preservation in laser microdissection and real-time reverse transcriptase-polymerase chain reaction. J Mol Diagn. 8:246–253.

Wang H, Qian WJ, Mottaz HM, Clauss TR, Anderson DJ, Moore RJ, Camp DG II, Khan AH, Sforza DM, Pallavicini M, et al. 2005. Development and evaluation of a micro- and nanoscale proteomic sample preparation method. J Proteome Res. 4:2397–2403.

Wood HM, Belvedere O, Conway C, Daly C, Chalkley R, Bickerdike M, McKinley C, Egan P, Ross L, Hayward B, et al. 2010. Using next-generation sequencing for high resolution multiplex analysis of copy number variation from nanogram quantities of DNA from formalin-fixed paraffin-embedded specimens. Nucleic Acids Res. 38:e151.